Turbulent Shearing of Crude Oil Mixed with Dispersants Generates Long Microthreads and Microdroplets

Balaji Gopalan and Joseph Katz

Department of Mechanical Engineering, Johns Hopkins University, Baltimore, Maryland 21218, USA
(Received 2 July 2009; published 1 February 2010)

Using cinematic digital holography, we demonstrate that turbulent breakup of crude oil mixed with dispersants into microdroplets starts with the formation of very long and quite stable, single or multiple microthreads that trail behind 300–1400 μm droplets. These threads extend from Reynolds number dependent regions with high surfactant concentration, which, along with associated viscosities and stretching by turbulence stabilizes the threads. The subsequent breakup, producing 2.8 μm droplets, is due to an increasing surface area and diffusion of dispersants into the continuous phase.

The addition of dispersants, oil and water soluble surfactants, lowers the interfacial tension between oil and water thereby accelerating the breakup of oil spills into droplets by the action of oceanic turbulence [1]. These droplets are dispersed by the fluid and are subsequently biodegraded. The small droplet sizes resulting from the addition of dispersants significantly increase the interfacial area available to the marine organisms, thereby accelerating the rate of biodegradation as long as they are not toxic to these organisms [2,3]. The current experimental study examines the effect of dispersants on the breakup of oil droplets and film, in an attempt to explain the formation of micron size droplets and a bimodal distribution of droplet sizes observed in experiments that simulate oil spill breakup [4].

The breakup of a cylinder of immiscible fluid due to the so-called capillary instability was first shown by Rayleigh [5]. Its dependence on flow conditions and fluid properties was subsequently characterized by Hinze [6]. In a laminar flow, droplet breakup requires that the capillary number, $\mu_c GD/\sigma$, exceeds a critical value, which depends on the viscosity ratio, μ_d/μ_c, and flow conditions [7]. Here μ is dynamic viscosity, G is strain rate, D is droplet diameter (measured along the major axis in the current paper), σ is interfacial tension and the subscripts c and d refer to disperse and continuous phases. In turbulent flows droplet breakup typically occurs when the Weber number (We), $\rho u^{*2}D/\sigma$, exceeds a critical value, whose magnitude is scattered over a wide range [8]. Here ρ is density and u^* is characteristic velocity. The effect of disperse phase viscosity is quantified by the Ohnesorge number (Oh), $\mu_d/(\rho_d D\sigma)^{0.5}$, whose increase raises the critical Weber number [9].

High disperse or continuous phase viscosity along with the surfactants may delay the pinch-off, resulting in formation of extended segments, threads, that remain attached to the droplet. Doshi *et al.* [10] injected a droplet into a quiescent medium with higher viscosity, and demonstrated formation of short lived, 8 μm radius, threads connecting the droplet to the needle. The same phenomenon, but

involving a high droplet viscosity, was reported by Zhang and Basaran [11]. Short lived threads attached to droplets were also seen by Vukasinovic *et al.* [12] during ultrasonic atomization of a high viscosity droplet. Numerical simulations by Jin *et al.* [13] showed that increasing surfactant concentration should cause formation of threads attaching droplet to needles. Another mode of thread formation from a droplet, typically referred to as tip streaming, occurs when a section of the immiscible fluid is extended into a conical shape due to: (i) accumulation of surfactants [14], (ii) shearing by coflowing liquid [15], and (iii) electrohydrodynamic forcing [16]. Microdroplets are formed when the tip of the cone extends and then breaks up. However, to the best of our knowledge, no study has reported the formation of long, stable, and (sometimes) multiple microthreads trailing behind droplets advected in a turbulent flow.

In this experiment we use Alaskan North Slope (ANS) crude oil premixed with the dispersant COREXIT 9527, from Nalco Energy Services, at dispersant to oil volumetric ratio (DOR) of 1:20 to 1:15. The continuous medium is filtered tap water at 20 °C, with a kinematic viscosity (ν) of 10^{-6} m^2/s. Measured values of specific gravity, viscosity, and surface tension of the mixtures with water are available in Table I. The surface tension for lower dispersant concentrations, DOR of up to 1:20, is measured from the height difference required to transform a flat surface of the mixture, at the end of a capillary tube immersed in water, into a hemisphere. For higher DOR, the surface tension is estimated from the oblateness and quiescent rise rate of the droplet (U_q), following Hu *et al.* [17].

In order to decouple the effect of droplet injection and breakup, we use a 0.15 mm (inner diameter) hypodermic needle to inject a mixture with DOR of 1:15, the concentration required for repeatable thread formation, into a nearly quiescent glass tube which lies within the turbulent facility. The mixture injection rate through the needle is adjusted so that the droplets are formed via a dripping mode [11]. Subsequently, the droplets rise up into a nearly homogeneous, stationary, and isotropic turbulent flow gen-

TABLE I.   Measured properties of the present ANS crude oil when it is mixed with the dispersant COREXIT 9527.

	Specific gravity ($\rho_c = 1000$ kg/m^3)	Kinematic viscosity (mm^2/s)	Surface tension (mN/m)	Ca* ($u' = 4.63$ cm/s)
Crude oil	0.847	7.1 ± 0.08	16.7	0.007
DOR 1:20	0.851	8.99	0.69	0.19
DOR 1:18.2	0.852	9.25	0.63	0.21
DOR 1:15.2	0.853	9.60	0.16	0.83

erated by four symmetrically spinning grids located at corners of a rectangular water tank that generates a high turbulence level with a very low mean velocity [18,19]. Consequently, droplets remain in the sample volume for an extended period. The turbulent characteristics in the facility, near the central region, have been carefully measured using 2D PIV at several planes and two perpendicular orientations, at all relevant experimental conditions. For the turbulent condition at which the bulk of the data have been obtained, the mean velocity is ~12% of the root mean square of fluid velocity fluctuations ($u' = 4.63$ cm/s), the turbulence kinetic energy dissipation rate (ε) is 19 cm^2/s^3, the Kolmogorov length scale [$\eta = (\nu^3/\varepsilon)^{0.25}$] is 151 μm and the integral length scale ($L = u'^3/\varepsilon$) is 5.2 cm [19]. The droplet motion is observed in a $1.7 \times 1.7 \times 7$ cm^3 sample volume, located at the center of the tank, using high-speed inline digital holography. The optical setup consists of a collimated laser beam illuminating the sample volume. The interference pattern between the light scattered from droplets and the remaining part of the illuminating beam is recorded by a high-speed $1k \times 1k$ camera at 500 frames/s. The reconstruction of the recorded holograms, plane by plane in the beam axis direction [19,20], brings all the objects, located within the "depth of focus," to come into focus. The observations are performed at different distances from the exit of the tube. At this turbulent level, breakup of 0.3–1.4 mm droplets (We, $\rho_d u'^2 D/\sigma$, $= 3.5$–16 and Oh $= 1.28$–0.58) due to capillary instability [21], which is demonstrated in Fig. 1, occurs infrequently.

Shortly after entering the turbulent domain, droplets larger than ~0.9 mm have a series of short threads extending from ~110° to 135° with respect to their leading edge [Fig. 2(a)], decreasing with increasing Weber number (droplet oblateness). Smaller droplets, about 0.6 mm and

smaller, typically have a single thread extending from their tail [Fig. 2(c)]. After a brief period (0.02–0.15 s) one or more of these threads extends into a substantial length (l), Fig. 2(b), reaching $l/D \approx 14$. The length scale of the threads becomes comparable to the turbulent integral length scale, while the thickness (d) rapidly becomes smaller than the present spatial resolution of our holographic system (17 μm). Occasionally, a segment of the long thread pinches off, and the section that remains attached does not retract completely, due to the low surface tension and high viscosity, and eventually starts stretching again along with the formation of additional threads. The pinched section is subsequently advected away by the turbulent flow. In some cases simultaneous multiple threads are pulled from the same droplet [Figs. 2(d) and 2(e)]. Slip of the buoyant oil droplets relative to the
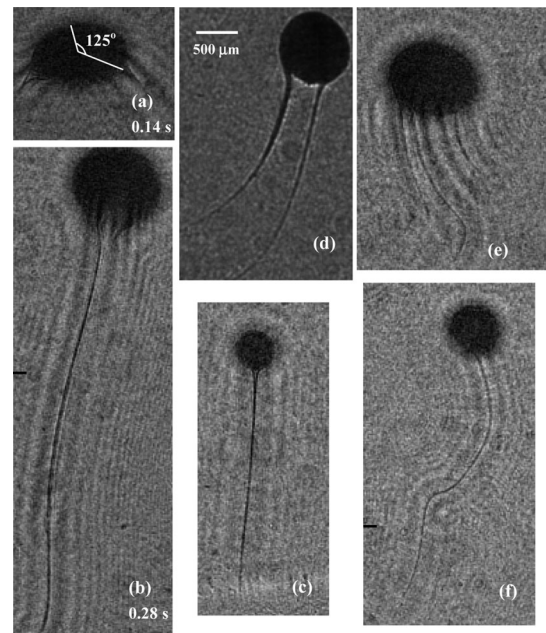
FIG. 2.   Reconstructed holograms of threads extending from crude oil droplets for DOR of 1:15 shown at the same magnification. (a) Threads extending at ~125° from the leading edge, 0.14 s after the droplet enters the turbulent flow, $D = 1.17$ mm. (b) The same droplet 0.14 s later, after stretching of the thread by the turbulent flow. (c) A single thread extending at 180° from a 0.46 mm droplet. (d) and (e) Multiple threads stretched from 0.85 and 1.07 mm droplets. (f) A twisted thread extending from a 0.6 mm droplet. Black bar indicates the boundary between two image sections of adjacent domains, which are reconstructed at different depth to keep the thread in focus.
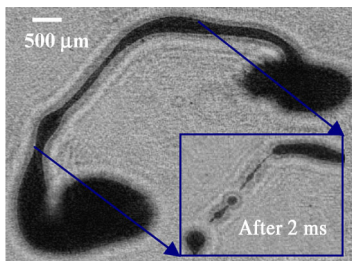

FIG. 1 (color online).   Reconstructed holographic images showing turbulent stretching of a crude oil droplet for DOR of 1:20, with inset showing the capillary breakup of a section 2 ms later.

local flow [18] stretches the thin threads initially. As their length becomes comparable to L, turbulence induced differences in the local velocity along the length of the thread deforms it [Fig. 2(f)] and extends it further. Consequently, the measured rate of stretching (1–7 cm/s), is of the same order as u'.

To understand the process of thread formation and separation, we have also injected the mixture into quiescent water and observed their behavior using inline digital holographic microscopy [20], at a resolution of 1.4 and 1.7 μm. Holograms are recorded at 15 frames/s using a $2k \times 2k$ digital camera and at 60–250 frames/s by a $1k \times 1k$ camera. A single thread extending behind a 0.43 mm droplet is evident in Fig. 3(a) for DOR of 1:15. Reducing the DOR to 1:18 to stop the thread formation and increasing the droplet size to ~2.1 mm generates the flow pattern shown in Fig. 3(b), as the surfactant is entrained by the flow around the droplet. Clearly, flow separation occurs at 124°, and near the separation point, the surface of the droplet is sheared towards the separation point from both directions, by the attached flow upstream and the reverse flow within the separated region downstream. Such a flow concentrates the surfactant near the separation region and reduces the local surface tension in a process similar to tip streaming in extensional flows [7], making them susceptible to thread formation. As the droplet Reynolds number ($U_q D/\nu$) decreases below 10, i.e., for droplets smaller than 0.6 mm, the separated region disappears. Consequently, for such small
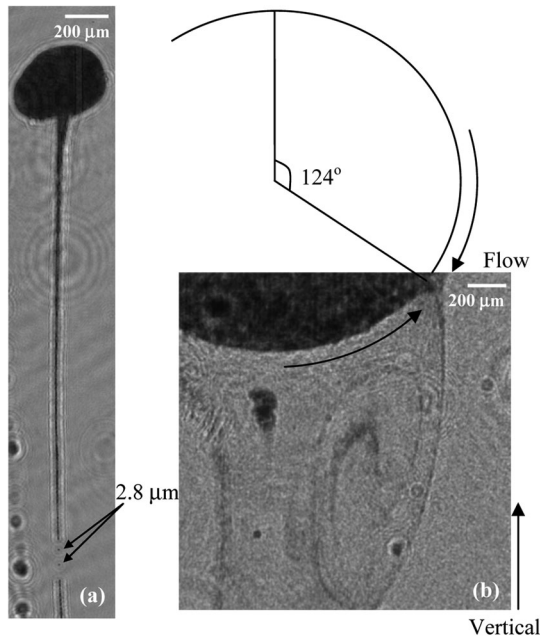

FIG. 3.   Crude oil droplets mixed with dispersant rising in a quiescent domain. (a) A 0.43 mm droplet with DOR of 1:15. The thread breaks up to form two 2.8 μm droplets, which are indicated by arrows. (b) Part of a 2.1 mm droplet with DOR of 1:18 and *without* oil shedding, showing that dispersant emerges from the droplet at the point of boundary layer separation, and is entrained into its wake.

droplets the surfactants is sheared towards the tail of the droplet (180°), resulting in formation of a single thread [Fig. 2(c)]. Differences between the threshold of Reynolds number for separation in comparison to that of solid spheres, observed by Taneda [22], is most likely a result of droplet deformation. It seems that thread formation occurs due to localized increase in concentration of surfactant, but the location of high concentration varies with Reynolds number and Weber number, the latter through shape deformation. This explanation can be extended to the turbulent flow, as shown subsequently.

The capillary number based on the droplet size ($D \sim$ 1 mm), strain rate associated with the turbulent flow, $G \sim (\varepsilon/\nu)^{0.5}$ [23], and bulk mixture properties is ~0.27, i.e., sufficient to deform the droplet and cause breakup, even with the presently high viscosity ratio [7]. However, exposure to such shear is intermittent and associated breakup is rare, because of the unsteady nature of turbulence and migration of the droplet relative to the local flow. On the other hand, the capillary number is higher in regions where flow separation causes accumulation of surfactants, both due to the low surface tension and high local shear, causing the formation of threads seen in Fig. 2. The effect of high droplet viscosity, low surface tension, and turbulence shearing in stabilizing the threads [7,24] can also be quantified using a modified capillary number, $Ca^* = (\mu_c \mu_d)^{0.5} u'/\sigma$ (see values in Table I), which has been used successfully by Gañán-Calvo *et al.* [25,26] to determine the stability of thin threads in coflowing liquids. Interestingly, we find that when $Ca^* = 0.007$–0.21, i.e., lower than or close to the threshold level for coflowing liquids [25,26], the thin threads do not develop. However, for $Ca^* = 0.83$, i.e., exceeding the threshold value, threads are observed extensively and repeatedly.

As the threads stretch, the increasing surface area decreases the surfactant concentration at the interface. Furthermore, diffusion of surfactants into the water becomes significant when the diameter of the thread becomes comparable to the molecular diffusion length scale $(D_m l/u')^{0.5}$, where D_m is the molecular diffusion coefficient. Using $D_m \sim 10^{-9}$ m^2/s and $l \sim 7$ mm, the diffusion length scale is ~12 μm, i.e., comparable to a typical thread diameter. Hence one should expect significant diffusion away from the droplet and a reduction in surfactant concentration. Consequently, the surface tension rises, making the thread prone to capillary instability. In the quiescent case, breakup of a thread section produces droplets as small as 2.8 μm diameter [Fig. 3(a)]. To determine whether such instabilities occur in the turbulent flow, we examine available holograms obtained at high turbulence levels ($\varepsilon = 256$ cm^2/s^3, $u' = 9.4$ cm/s, $Ca^* = 0.38$), where the wavy surface of threads [Fig. 4(a)] provides clear evidence of capillary instabilities. Another possible mode of thread breakup involves thread contraction. Conditions for contraction and related breakup depends on the local Ohnesorge number (Oh_d), $\mu_d/(\rho_d d\sigma)^{0.5}$, based on the bulk mixture properties and thread diameter
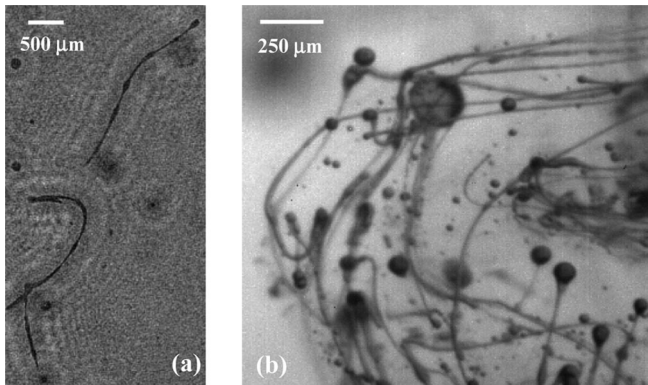
FIG. 4. (a) Reconstructed hologram showing capillary waves on the surface of detached oil threads with initial DOR of 1:20 at a high turbulence level ($\varepsilon = 256$ cm^2/s^3, $u' = 9.4$ cm/s). (b) Image of droplets with long threads trailing behind them, which are produced when a water jet impinges on a surface layer of oil mixed with dispersant (DOR = 1:15).

($d \sim 10^{-5}$ m). Its value, ~ 7, is a very large number [27]. Hence, significant contraction of the threads and its associated instabilities do not occur in our case. However, we do see the threads contracting partially after a breakup, suggesting that locally the Oh$_d$ decreases to a sufficiently low level.

To confirm that the thread formation and subsequent breakup indeed plays a role in breakup of oil surface layer, we establish a ~ 2–3 mm layer of oil with DOR of 1:15, on the surface of quiescent water. The interface is impinged with a ~ 3–4 mm diameter water jet at a velocity of 0.4–0.7 m/s, i.e., comparable to typical breaking wave velocity [28]. The resulting process is observed by high-speed shadowgraphy, at a spatial resolution of 5.6 μm. As shown in Fig. 4(b), jet impingement and associated downward fluid motion entrains oil from the surface, resulting in formation of numerous droplets with threads extending from them. Subsequent residual flows keeps on stretching these threads and generating new ones long after the initial impingement. Experiments by Li *et al.* [4] on the breakup of oil film treated with dispersants have shown that wave breaking produces a bimodal distribution of droplet sizes with peaks at 1 and 150 μm. We believe that the presently observed thread formation, which seems to depend on Ca*, explains the 1 μm peak, while the larger droplets are a result of capillary instability among other phenomena.

In conclusion, shearing of a crude oil droplet mixed with dispersants, and resulting formation of localized regions with low surface tension produces very long, micron sized oil threads that trail behind the droplets. The shearing may be caused by interaction with turbulence, including that caused by the breaking waves, or simple buoyant rise. The point of thread extension from the surface depends on the droplet Reynolds number. Associated Ca* exceeds the threshold level needed for maintaining thread stability owing to high turbulence, low surface tension, and viscosi-

ties involved. Eventual breakup of these threads to micron sized droplets occurs due to presumed reduction of surfactant concentration, as the surface area increases and the water soluble dispersant diffuses into the surrounding fluid.

[1] M. Li and C. Garrett, Mar. Pollut. Bull. **36**, 961 (1998).
[2] R. R. Lessard and G. Demarco, Spill Sci. Technol. Bull. **6**, 59 (2000).
[3] G. J. Mulkins-Philips and J. E. Stewart, Appl. Environ. Microbiol. **28**, 547 (1974).
[4] Z. Li, P. Kepkay, K. Lee, T. King, M. C. Boufadel, and A. D. Venosa, Mar. Pollut. Bull. **54**, 983 (2007).
[5] Lord Rayleigh, Philos. Mag. **34**, 145 (1892).
[6] J. O. Hinze, AIChE J. **1**, 289 (1955).
[7] H. A. Stone, Annu. Rev. Fluid Mech. **26**, 65 (1994).
[8] A. Wierzba, Exp. Fluids **9**, 59 (1990).
[9] D. D. Joseph, J. Belanger, and G. S. Beavers, Int. J. Multiphase Flow **25**, 1263 (1999).
[10] P. Doshi, I. Cohen, W. W. Zhang, M. Siegel, P. Howell, O. A. Basaran, and S. R. Nagel, Science **302**, 1185 (2003).
[11] X. Zhang and O. A. Basaran, Phys. Fluids **7**, 1184 (1995).
[12] B. Vukasinovic, M. K. Smith, and A. Glezer, Phys. Fluids **19**, 012104 (2007).
[13] F. Jin, N. R. Gupta, and K. J. Stebe, Phys. Fluids **18**, 022103 (2006).
[14] S. L. Anna and H. C. Mayer, Phys. Fluids **18**, 121512 (2006).
[15] R. Suryo and O. A. Basaran, Phys. Fluids **18**, 082102 (2006).
[16] R. T. Collins, J. J. Jones, M. T. Harris, and O. A. Basaran, Nature Phys. **4**, 149 (2008).
[17] Y. T. Hu, D. J. Pine, and L. Gary Leal, Phys. Fluids **12**, 484 (2000).
[18] P. D. Friedman and J. Katz, Phys. Fluids **14**, 3059 (2002).
[19] B. Gopalan, E. Malkiel, and J. Katz, Phys. Fluids **20**, 095102 (2008).
[20] J. Sheng, E. Malkiel, and J. Katz, Appl. Opt. **45**, 3893 (2006).
[21] C. D. Eastwood, L. Armi, and J. C. Lasheras, J. Fluid Mech. **502**, 309 (2004).
[22] S. Taneda, J. Phys. Soc. Jpn. **11**, 1104 (1956).
[23] Y. Zhu and R. A. Antonio, Appl. Sci. Res. **57**, 337 (1996).
[24] J. Eggers and E. Villermaux, Rep. Prog. Phys. **71**, 036601 (2008).
[25] A. M. Gañán-Calvo, R. González-Prieto, P. L. Riesco-Chueca, M. A. Herrada, and M. Flores-Mosquera, Nature Phys. **3**, 737 (2007).
[26] A. M. Gañán-Calvo, Phys. Rev. E **78**, 026304 (2008).
[27] P. K. Notz and O. A. Basaran, J. Fluid Mech. **512**, 223 (2004).
[28] K.-A. Chang and P. L.-F. Liu, Phys. Fluids **11**, 3390 (1999).